Acta Biomaterialia xxx (xxxx) xxx

Contents lists available at ScienceDirect

Acta Biomaterialia

journal homepage: www.elsevier.com/locate/actbio

Full length article

Probing prodrug metabolism and reciprocal toxicity with an integrated and humanized multi-tissue organ-on-a-chip platform

Shiny Amala Priya Rajan[a,b], Julio Aleman[a], MeiMei Wan[a], Nima Pourhabibi Zarandi[a], Goodwell Nzou[a], Sean Murphy[a], Colin E. Bishop[a], Hooman Sadri-Ardekani[a], Tom Shupe[a], Anthony Atala[a], Adam R. Hall[a,b,c,**], Aleksander Skardal[a,b,c,d,e,*]

[a] Wake Forest Institute for Regenerative Medicine, Wake Forest School of Medicine, Medical Center Boulevard, Winston-Salem, NC 27157, USA
[b] Virginia Tech –Wake Forest School of Biomedical Engineering and Sciences, Wake Forest School of Medicine, Medical Center Boulevard, Winston-Salem, NC 27157, USA
[c] Comprehensive Cancer Center of Wake Forest Baptist, Wake Forest Baptist Medical Center, Medical Center Boulevard, Winston-Salem, NC 27157
[d] Department of Biomedical Engineering, The Ohio State University, 1080 Carmack Rd., Columbus, OH 43210
[e] The Ohio State University Comprehensive Cancer Center, The Ohio State University Wexner Medical Center, 460 W 10th Ave, Columbus, OH 43210

ARTICLE INFO

Article history:
Received 20 November 2019
Revised 11 February 2020
Accepted 11 February 2020
Available online xxx

Keywords:
Tissue chip
Organ-on-a-chip
Organoid
Drug response
Drug metabolism

ABSTRACT

Current drug development techniques are expensive and inefficient, partially due to the use of preclinical models that do not accurately recapitulate *in vivo* drug efficacy and cytotoxicity. To address this challenge, we report on an integrated, *in vitro* multi-organoid system that enables parallel assessment of drug efficiency and toxicity on multiple 3D tissue organoids. Built in a low-cost, adhesive film-based microfluidic device, these miniaturized structures require less than 200 µL fluid volume and are amenable to both matrix-based 3D cell culture and spheroid aggregate integration, each supported with an *in situ* photocrosslinkable hyaluronic acid hydrogel. Here, we demonstrate this technology first with a three-organoid device consisting of liver, cardiac, and lung constructs. We show that these multiple tissue types can be kept in common circulation with high viability for 21 days and validate the platform by investigating liver metabolism of the prodrug capecitabine into 5-fluorouracil (5-FU) and observing downstream toxicity in lung and cardiac organoids. Then we expand the integrated system to accommodate six humanized constructs, including liver, cardiac, lung, endothelium, brain, and testes organoids. Following a 14-day incubation in common media, we demonstrate multi-tissue interactions by metabolizing the alkylating prodrug ifosfamide in the liver organoid to produce chloroacetaldehyde and induce downstream neurotoxicity. Our results establish an expandable, multi-organoid body-on-a-chip system that can be fabricated easily and used for the accurate characterization of drug interactions *in vitro*.

Statement of Significance

The use of 3-dimensional (3D) *in vitro* models in drug development has advanced over the past decade. However, with several exceptions, the majority of research studies using 3D *in vitro* models, such as organoids, employ single tissue types, in isolated environments with no “communication” between different tissues. This is a significant limiting factor because in the human body there is significant signaling between different cells, tissues, and organs. Here we employ a low-cost, adhesive film-based microfluidic device approach, paired with a versatile extracellular matrix-derived hyaluronic acid hydrogel to support integrated systems of 3 and 6 3D organoid and cell constructs. Moreover, we demonstrate an integrated response to drugs, in which downstream toxicity is dependent on the presence of liver organoids.

* Corresponding author, Aleksander Skardal, Department of Biomedical Engineering, Tzagournis Medical Research Facility, Suite 514A, 420W. 12th Ave. Columbus, OH 43210, USA
** Co-Corresponding author, Adam R. Hall, Department of Biomedical Engineering, Biotech Place, 575N. Patterson Ave., Suite 120, Winston-Salem, NC 27101, USA.
E-mail addresses: arhall@wakehealth.edu (A.R. Hall), skardal.1@osu.edu (A. Skardal).

https://doi.org/10.1016/j.actbio.2020.02.015
1742-7061/

1. Introduction

A key challenge for the pharmaceutical industry is the lack of predictive models for drug discovery and toxicity testing. From the compound/drug development stage, only about 10% of drugs achieve FDA approval in clinical trials and are subsequently effective in humans [1,2]. Most failures occur in heavily invested-in phase III trials and could be mitigated with superior drug testing models [3]. The current drug development process is heavily reliant on inefficient 2D cell cultures and expensive and time-consuming animal models. However, these preclinical models largely fail to either recapitulate human physiology or the structural and functional complexity of tissues and organs. For example, static 2D *in vitro* models are often composed of single cell types, which is not representative of a functional multicellular tissue. On the other hand, while animal models represent a complete and integrated system, differences in drug metabolism and cellular response to chemical signals relative to humans [4] make their predictive accuracy debatable. 3D cell culture models are known to mimic the mechanical, chemical, and physiological properties of *in vivo* tissue better than simple 2D models and can contain heterogeneous human cells to provide relevant assessments [5,6]. Though some 3D models such as organoids can faithfully represent some aspects of *in vivo* tissues, their isolated and often static nature coupled with the typical use of a single drug dose does not reproduce complex multi-organ intercommunication through metabolite and chemical exchange or *in vivo* pharmacokinetics of drug delivery. Consequently, there is a critical need to develop dynamic systems with physiologically relevant tissue models and controlled spatiotemporal media conditions to better model drug and organ interactions.

Integrating 3D cell culture constructs with microfluidics provides the capability to control dynamic factors of the microenvironment with spatial precision and supports the introduction of mechanical and chemical cues missing in static 3D models. These minimalist microfluidic constructs represent key organ-level structural, functional, and mechanical properties and are collectively referred to as organ-on-a-chip systems. As functional *in vitro* units of organs that display highly accurate biological response analogous to *in vivo* systems, organ-on-a-chip technologies have been an emerging interest for a decade [7–12]. Such systems have targeted well-known drug challenges to further support platform efficacy for drug discovery processes [10,12–17], especially in the preclinical phase. However, single-organoid platforms lack the complex and interactive nature of the human body, and consequently fall short of replicating systemic drug interactions. To partially capture *in vivo* intricacy, multiple microphysiological systems can be integrated and maintained under a common media to promote interactions between organs and study drug effects [18–20]. These body-on-a-chip (BOC) devices represent physiologically-based pharmacokinetic models that can simulate recirculation in a closed system. Furthermore, they can be designed not only to reproduce relative organ sizes [21] and liquid-to-organ volume ratios [17,22] faithfully, but can also generate realistic concentration dynamics for each tissue compartment and emulate temporal dose changes [23] in a more consistent and controlled manner than can be achieved in alternative platforms.

There have been various approaches to realize BOC systems integrating multiple organs [19,20,24–28]. A primary concern in these efforts is the development of a complete common media that can support the multiple cell types incorporated in different organoids [22,29]. Compared to cell line-based BOCs that can often employ simple media formulations [30,31], BOC systems with primary cells or induced pluripotent stem cells (iPSCs) can present additional challenges due to their individualized media needs. This weighs the need for integration of multiple organs against maintaining high viability and functionality of the organoids. A second obstacle arises from the materials used for microfluidic device fabrication. Traditionally, microfluidic chips are fabricated using polydimethylsiloxane (PDMS), which is biocompatible, optically clear, and allows passive gas exchange. However, because of its hydrophobic nature, PDMS can adsorb hydrophobic compounds, including many proteins and drugs [32] and can also allow for evaporation of liquid over long-term experiments. Consequently, it is critical to consider materials that will not alter the pharmacokinetic profiles of tested drugs or the concentrations of secreted macromolecules over long-term studies. A third challenge is production of a closed-circuit, unidirectional fluid flow between organoids that allows physiologically relevant volume ratios to be maintained. In addition to these central considerations, the system should also enable direct imaging and on-demand media access for analysis.

Here, we demonstrate a multi-tissue system containing organoids constructed entirely with human cells. We employ a straightforward and low-cost technique to build our microfluidic devices with biocompatible thermoplastic polymers [32] and then biofabricate functional spheroids or 3D cell-laden hydrogel constructs in them. The resulting system mimics basic circulatory and physiological aspects of the complex human body in a miniaturized format (30 μL per organoid chamber) using 3 or 6 discrete tissues collectively composed of up to 20 different cell types, including primary and iPS-derived cells. We maintain these integrated constructs under a common circulating media for extended experimentation and challenge them by conducting drug studies in which prodrugs with no intrinsic reactivity are metabolized by a functional liver organoid to produce reactive metabolites that influence adjoining organoids. While still a simple distillation of complex human physiology, the system described herein offers an easy-to-fabricate multi-tissue platform to begin to explore complex drug and toxin interactions between tissue types *in vitro*.

2. Experimental methods

2.1. Fabrication of adhesive film-based multi-tissue chips

The adhesive film-based (AFB) microfluidic chip was fabricated with a low-cost technique that uses rapid-prototyping of patterned adhesive films [16]. The channels in these chips were formed with a computer-controlled razor plotter (CE6000-40, GraphTec, Irvine, CA) in a double-sided adhesive film (140 μm thickness, part number 3M9495MPF, Strouse, Westminster, MD) employing engineered perforations between each layer to aide self-alignment (Fig. 1a). Channels consisting of multiple adhesive film layers were essential to accommodate the varying sizes of functional spheroids, ranging from 150 μM to 500 μM in diameter. Hence, each microfluidic chip consisted of 4 layers of adhesive film for the 3- and 6-organoid systems to produce a channel height of 560 μM. The 3- and 6-organoid systems had similar fabrication approaches, except for a slightly modified channel design: the 3-organoid design featured 3 discrete chambers (3 mm in diameter) connected in series by external tubing (Fig. 1b, right top) whereas the 6-organoid design was optimized to form 5 internally-connected chambers (4 mm in diameter) as well as one additional 4 mm chamber connected to the rest of the system via external tubing (Fig. 1b, right bottom). This design was tailored to accommodate the optional integration of one organoid (liver) that could be removed from the circulation for comparative studies. The multi-layered patterned films were securely adhered to a glass microscope slide (VWR, Radnor, PA) to facilitate direct imaging. All organoids were then biofabricated in the designated chambers (see *In situ patterning of organoids*) and the top side was firmly sealed using a PMMA (1/8″ thickness, McMaster-Carr, Elmhurst, IL) lid cut to the slide dimensions

Please cite this article as: S.A.P. Rajan, J. Aleman and M. Wan et al., Probing prodrug metabolism and reciprocal toxicity with an integrated and humanized multi-tissue organ-on-a-chip platform, Acta Biomaterialia, https://doi.org/10.1016/j.actbio.2020.02.015

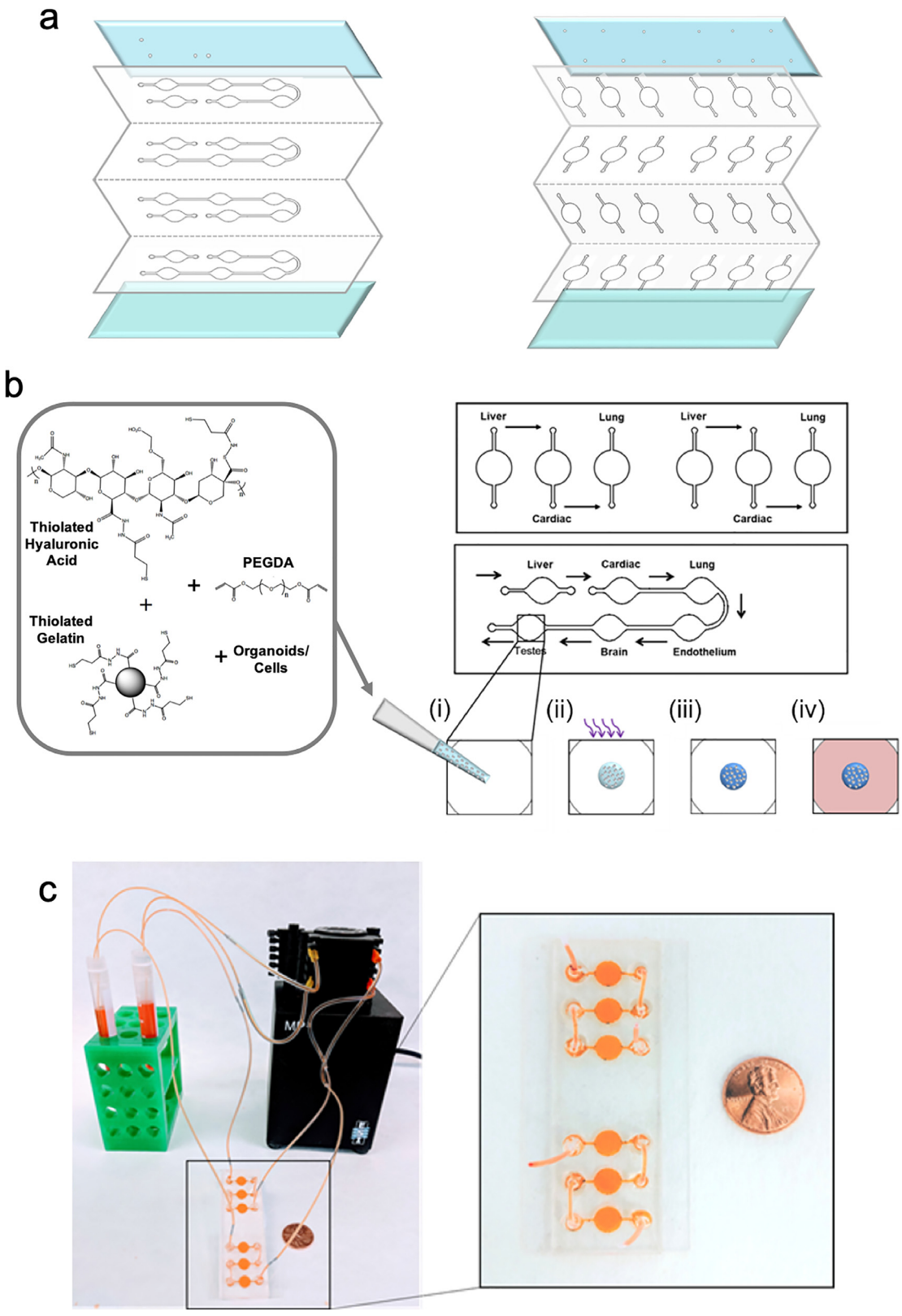

Fig. 1. *In situ* photopatterning of multiple organ-specific tissue. (a) Schematics of microfluidic device layers for the AFB 3-organoid (left) and 6-organoid (right) platform. (b) *In situ* organoid patterning technique using a hydrogel comprised of thiolated hyaluronic acid, thiolated gelatin, PEGDA, and a photoinitiator: in a microfluidic chamber *(i)* the hydrogel mixture containing HA hydrogel, photoinitiator, and organ-specific spheroid/cells are pipetted as a drop (light blue) and then illuminated with UV light directly *(ii)*. Exposed precursor is crosslinked into a hydrogel (dark blue), encapsulating spheroids or cells within the region *(iii)*. Finally, common media formulation (red) is added to the chamber for incubation *(iv)*. (c) The total measurement set-up, featuring a low-volume, closed-loop fluidic circuit for each organoid system facilitated by a computer-controlled peristaltic pump. (For interpretation of the references to colour in this figure legend, the reader is referred to the web version of this article.)

Please cite this article as: S.A.P. Rajan, J. Aleman and M. Wan et al., Probing prodrug metabolism and reciprocal toxicity with an integrated and humanized multi-tissue organ-on-a-chip platform, Acta Biomaterialia, https://doi.org/10.1016/j.actbio.2020.02.015

Table 1
A summary of each organoid or tissue construct type with the cells making them up. Also described are the various cell sources and cell types (primary, cell line, iPSC-derived, etc.), relative percentage in each model, and documented tissue specific functionalities.

Organoid or tissue construct type	Cell types	cell source	Type of cell	Percentage in model	Documented functionality	Citation
Liver	Hepatocytes	Bioreclamation	Primary human	75%	Albumin and urea secretion; Drug metabolism; Toxicity responses	[18,47]
	Stellate cells	Bioreclamation	Primary human	10%		
	Kupffer cells	Sekisui XenoTech	Primary human	10%		
	Liver-Derived endothelial cells	Lonza	primary human	5%		
Cardiac	Cardiomyocytes	Ncardia	iPSC	75%	Spontaneous beating; Beating changes in response to drugs; Toxicity responses	[18,47]
	Cardiac fibroblasts	ScienCell	Primary HUMAN	20%		
	Cardiac endothelial cells	ScienCell	Primary human	5%		
Lung (3-tissue system)	A549 Alveolar epithelial cells	Lonza	Human cell line	100%	n/a	–
Lung (6-tissue system)	Lung fibroblasts	Lonza	Primary human	20%	n/a	–
	Human bronchial epithelial cells	Lonza	Primary human	80%		
Endothelial	HUVEC	Lonza	Primary human	100%	n/a	–
Testis	Spermatogonial stem cells	Donor via NDRI	Primary human	~80%	Androgen production; Supporting germ cell differentiation; Toxicity responses; Virus replication	[34-36]
	Leydig cells	Donor via NDRI	Primary human	~10%		
	Sertoli cells	Donor via NDRI	Primary human	~10%		
	Peritubular cells	Donor via NDRI	Primary human	Contaminant of SSC populations		
Brain	Brain microvascular endothelial cells	Cell Systems	Primary human	30%	Barrier function to the middle of the spheroid	[37]
	Brain vascular pericytes	ScienCell	Primary human	15%		
	Astrocytes	ScienCell	Primary human	15%		
	Microglia	Tempo Bioscience	IPSC	5%		
	Oligodendrocytes	Tempo Bioscience	Oligodendrocyte progenitor cells	15%		
	Neural cells	Axol Biosciences	Neural stem cells	20%		

and furnished with ports using a laser etcher (Full Spectrum Laser H-series, Las Vegas, NV). The ports were fitted with polytetrafluoroethylene (PTFE) tubing (0.022″ID × 0.042″ID, Cole Parmer, Vernon Hills, IL) and secured using a UV-cure polyester resin (Solarez, Vista, CA).

2.2. Cell sources, culture, and organoid formation

Note that the nomenclature used to define spheroids, organoids, and 3D tissue constructs varies between research groups as well as between fields of biomedical research. Here, spheroids refer to cellular constructs formed without an extrinsic hydrogel scaffold via approaches like the hanging drop method, in which cells self-assemble and form native cell-cell and/or cell-ECM junctions internally. Organoids refer to any cellular construct having specific organ-like function, and thus include both spheroids and scaffold-supported mixtures of individual cells consisting of multiple cell types designed to emulate organ complexity. The term 3D tissue construct refers to a fabricated 3D hydrogel scaffold structure containing individual cells or cells in spheroid form. Cell sources and relative contributions to each organoid or tissue construct type are described in Table 1.

2.2.1. Liver constructs

Primary human hepatocytes (HH, Bioreclamation VT, Westbury, NY) were thawed in human cryopreserved hepatocyte thawing media (MCHT50, Lonza, Morristown, NJ) as per manufacturer instructions and transferred to hepatocyte culture media (CC-3198, HCM; Lonza) in 50 mL conical tube. This cell suspension was centrifuged and the resulting pellet collected for immediate use. Both hepatic stellate cells (HSc, Bioreclamation VT) and Kupffer cells (HK1000.H15, Sekisui XenoTech, Kansas City, KS) were obtained frozen, thawed in 37 °C water bath, and used immediately. Human liver-derived endothelial cells (HLEc) (HLECP2, Lonza) were expanded with minimal passaging and cultured in endothelial cell growth media (EGM™) (CC-3124, Lonza) with 10% fetal bovine serum (FBS) (S11050, Atlanta Biologicals, Flowery Branch, GA) and other supplements provided by the manufacturer and then cryopreserved until use. Except HH, all cell types were thawed and centrifuged to form a cell pellet that was used directly in experiments. Compositions of 75% HH, 10% HSc, 10% Kupffer cells, and 5% HLEc were prepared and then aggregated in a Corning® Costar® 96-well ultra-low adherent culture plates (CLS3474, Sigma Aldrich, St. Louis, MO, USA). Each well had approximately 2000 cells in the above-mentioned ratio per 100 µL of HCM (Lonza) with 20% FBS and 1000X dilute Gentamicin. They were then incubated and observed for formation of spheroids that were subsequently integrated into organoids (see *In situ patterning of organoids*).

Important considerations in our study and in other *in vitro* studies employing primary human hepatocytes are the limitations intrinsic to such cells, such as batch-to-batch variation and functional depreciation. Indeed, in our experience working with hepatocytes, we have found cell sourcing to be challenging, with new lots and different donors yielding variable functional results. Consequently, many studies incorporating the cell type can require frequent recharacterization, ultimately leading to lost productivity difficulty in planning. In the long term, it may be that iPSC-derived hepatocytes will be a superior and less limited cell source. But to date, these cells suffer from significant functional limitations of their own.

2.2.2. Cardiac constructs

Commercially sourced iPSc-derived cardiomyocytes (CM, Cor.4U®, Ncardia, Leiden, The Netherlands) were cultured on a Matrigel-coated (17 µL/mL of media; 354,234, Corning) six-well plate in Pluricyte® complete cardiomyocyte culture media (CCM; Ncardia) with 10% FBS and 1% penicillin-streptomycin (P/S). After a 24 h incubation, the complete media was renewed, and the cells were incubated until they began beating spontaneously (up

Please cite this article as: S.A.P. Rajan, J. Aleman and M. Wan et al., Probing prodrug metabolism and reciprocal toxicity with an integrated and humanized multi-tissue organ-on-a-chip platform, Acta Biomaterialia, https://doi.org/10.1016/j.actbio.2020.02.015

to 48 hrs). To facilitate efficient harvesting of CM cells, the plate was first washed with PBS and 0.5 M EDTA. Then the cells were detached from the plate with trypsin (0.25%; 215,310, Difco Laboratories, Detroit, MI) under mild agitation and used immediately. Both normal human cardiac fibroblast (NHCF) and cardiac endothelium cells (CE) were sourced commercially (6300 and 6000, ScienCell) and used as purchased after thawing to room temperature. A cell mixture was prepared consisting of 75% CM, 20% NHCF, and 5% CE and loaded into wells of a 96-well non-adherent round bottom plate (Sigma Aldrich) and incubated to aggregate in 100 µL of cardiomyocyte maintenance media (A2920802, Gibco/Thermo Fisher, Waltham, MA). Each well contained approximately 2500 cells. Well plates were observed regularly until spheroids fully developed and produced beating-like contractile movement. These were used directly in organoid formation (see *In situ patterning of organoids*).

2.2.3. Lung constructs

Alveolar epithelial cells (A549, CCL-195, ATCC, Manassas, VA) were expanded in a cell culture-treated flask (T-175, Thermofisher) and cultured in high glucose Dulbecco's Modified Eagle's media (DMEM; Thermofisher), 10% fetal bovine serum (FBS, Atlanta Biologicals), and 1% P/S. In the 3-organoid system, the lung construct was biofabricated as a suspension of these cells in polymerized hydrogel scaffold (see *In situ patterning of organoids*).

Normal Human Lung Fibroblast (CC-2512, NHLF, Lonza) were cultured and expanded in Alpha MEM (36,450, StemCell Technologies, Cambridge, MA), 10% FBS (Atlanta Biologicals) and 1% (P/S). The cells were harvested using 0.05% trypsin (Difco) prior to use. Primary Normal Human Bronchial Epithelial cells (CC-2540, NHBE, Lonza) were expanded in a culture flask coated with Type I Bovine Collagen (0.04 mg/ml, 804,592, Sigma Aldrich) in Bronchial Epithelial Cell Growth media (CC-3170, Lonza) with supplements provided by the manufacturer and 5 µM Y-27,632 (ROCK inhibitor, 72,304, StemCell Technologies). Irradiated primary lung fibroblast were used as feeder cells. NHBE and NHLF were mixed at a ratio of 4:1 and added to an ultra-low attachment U-bottom plate (Sigma-Aldrich) for aggregation in Organoid Formulation media (OFM) that consisted of complete DMEM with 20% FBS and rat tail collagen I (10 ng/µL; Corning). The plate was incubated at 37 °C and monitored daily for spheroid formation. Resulting spheroids were used in the 6-organoid system (see *In situ patterning of organoids*).

2.2.4. Blood vessel constructs

Human Umbilical Vein Endothelial Cells (HUVEC) (C2517A, Lonza) were expanded and maintained in EGM (Lonza) with 10% FBS and other supplements provided by the manufacturer prior to use. Only cells under passage five were used for experiments. The blood vessel construct was biofabricated as a suspension of these cells in polymerized hydrogel scaffold (see *In situ patterning of organoids*).

2.2.5. Testis constructs

Testis spheroids consisted of human primary testicular cells including spermatogonial stem cells (SSC), Leydig cells, Sertoli cells, and peritubular cells. These cells were sourced from the cryopreserved fragments of adult testicular tissues (whole organ) of brain-dead patients that were procured through the National Disease Research Interchange (NDRI). Note that while cells with *in vivo* barrier functions were used, barrier layers were not established in our constructs and so these functions were not considered. Briefly, human testicular cells were isolated and cultured from frozen tissue according to previously established methods [33–35] using the primary Sertoli, Leydig, and peritubular cells as the somatic feeder layer. Testicular cells were seeded and expanded up to 5–6 passages in a cell culture treated 75 cm^2 flask (Thermo Scientific) using enriched Stempro-34 media (10,639,011, Thermo Fisher) [35]. The spheroids were made by suspending the trypsin-treated cells in testicular spheroid formation media that was made from enriched StemPro-34, 30% FBS, and 1 µg/mL solubilized human testis ECM (derived as described previously) [35]. The cells were seeded to aggregate into 96-well format ultra-low attachment round bottom plates (7007, Corning) at a density of 10,000 cells/100 µL volume. Plates were then spun at 150 × *g* for 30 s to initiate and facilitate the aggregation process. After 48 h incubation, the compact spheroids were transferred into 96-well format ultra-low attachment U-bottom plates (Sigma-Aldrich) [36] and subsequently integrated (see *In situ patterning of organoids*).

2.2.6. Brain constructs

Brain spheroids were prepared as previously reported [37], consisting of six commercially-sourced human primary and iPSC-derived cell types: 30% primary human brain microvascular endothelial cells (HBMEC), 15% human brain vascular pericytes (HBVP), 15% human astrocytes (HA), 5% human microglial (HM), 15% human oligodendrocytes (HO), and 20% human neural (HN) cells. As above, while cells with *in vivo* barrier functions were used here, such layers were not established and thus barrier functions were not considered. HBMEC (ACBRI 376, Cell Systems, Kirkland, WA) were cultured and expanded in attachment factor-coated plate and incubated in complete classic media (4Z0-500, Cell Systems, Kirkland, WA) that was supplemented with CultureBoost™ and attachment factor (4Z0-201, Cell Systems). HBVP and HA cells (1200 and 1800, ScienCell Research Laboratories, Carlsbad, CA) were cultured and expanded in plates coated with Poly-L-Lysine (15 µg/ml; 0413, ScienCell Research Laboratories). HBVP cells were cultured in pericyte media (1201, ScienCell Research Laboratories) with 2% FBS, 1% pericyte growth supplement (1252, ScienCell Research Laboratories), and 1% penicillin-streptomycin. HA cells were cultured in astrocyte media (1801, ScienCell Research Laboratories) containing 2% FBS, 1% astrocyte growth supplement (1852, ScienCell Research Laboratories), and 1% penicillin-streptomycin. Human iPSC-derived microglia (Tempo-iMG, Tempo Bioscience Inc., San Francisco, CA) and HO progenitor cells (TempiOligo, Tempo Bioscience Inc.) were expanded in plates coated with Matrigel (0.2 mg/ml; Corning). HM cells were cultured in DMEM/F-12 (Life Technologies), supplemented with 0.5% essential amino acids (Life Technologies), 1% N2 supplement (Life Technologies), 2% L-glutamine (Life Technologies), GM-CSF (100 ng/mL, 300–03, Peprotech, Rocky Hill, NJ), and IL-34 (50 ng/mL, 200–34, Peprotech). HO cells were initially cultured in a propagation media and replaced by differentiation media 72 h prior to spheroid formation. Propagation media was made of DMEM/F12 supplemented with HEPES, 2 mM L-glutamine (Life Technologies), 1X non-Essential amino acids (Life Technologies), StemPro neural supplement (A1050801, Thermo Fisher), 10 ng/mL PDGF-AA (100–13A, Peprotech), 10 ng/mL PDGF-AB (100–00AB, Peprotech), 10 ng/mL NT3 (450–03, Peprotech), 100 ng/mL biotin (B4501, Sigma Aldrich), and 5 µM/mL cAMP (A9501, Sigma Aldrich). Differentiation media was made of 50% DMEM/F12 and 50% Neuralbasal (21,103,049, Thermo Fisher), and supplemented with 1X non-essential amino acids, 1x B27 (17,504,044, Thermo Fisher), 2 mM L-glutamine, 100 ng/mL biotin, 5 ng/mL PDGF-AA, 10 ng/ml BDNF (450–02, Peprotech), 20 µg/mL ascorbic acid (A4403, Sigma Aldrich), 1 µM/ml cAMP, and 200 ng/ml T3 (T6397, Sigma Aldrich). HN stem cells (ax0011, Axol Biosciences Ltd., Cambridge, UK) were cultured and expanded on plates coated with SureBond (ax0041, Axol Biosciences) in neural plating-XF media (ax0033, Axol Biosciences). After 24 hours, the media was replaced with neural expansion-XF media (ax0031, Axol Biosciences) with recombinant human 20 ng/mL FGF2 (ax0047, Axol Biosciences) and 20 ng/mL recombinant human EGF (ax0048, Axol Biosciences). After a suffi-

Please cite this article as: S.A.P. Rajan, J. Aleman and M. Wan et al., Probing prodrug metabolism and reciprocal toxicity with an integrated and humanized multi-tissue organ-on-a-chip platform, Acta Biomaterialia, https://doi.org/10.1016/j.actbio.2020.02.015

cient number of cells was achieved, neuronal phenotypic differentiation was ensured by replacing the expansion media with neural differentiation-XF media (ax0034, Axol Biosciences).

To make the spheroids, initially 1100 cells of HA, HN, HO and HM were aggregated in 96-well hanging drop culture plates (InSphero AG, Schlieren, Switzerland) in the ratio described above with 45% astrocyte media without astrocyte growth supplements, 45% neural maintenance-XF media, 10% heat-inactivated FBS (Thermo Fisher), and 10 ng/μL rat tail collagen I (Corning). After 48 h, the neuroglial organoid was subsequently coated with HBMEC and HBVP cells by adding them in the suspension media. These organoids were then cultured in 60% neural maintenance-XF media (aa0031, Axol Biosciences Ltd.), 20% astrocyte media (ScienCell Research Laboratories) and 20% complete classic media until they matured and then were transferred into a 96-well plate for subsequent use (see *In situ patterning of organoids*).

2.3. Extracellular matrix (ECM) hydrogel preparation

ECM-mimicking HA/gelatin-based hydrogel (HyStem-HP, ESI-BIO, Alameda, CA) was used as the 3D organoid scaffold and was prepared as previously described [38]. Briefly, a thiolated HA component (Glycosil®), a thiolated gelatin component (Gelin-S®), and polyethylene glycol diacrylate crosslinker (PEGDA, Extralink®) were dissolved separately in sterile water containing 0.05% w/v of the photoinitiator 2-Hydroxy-4′-(2-hydroxyethoxy)−2-methylpropiophenone (410,896, Sigma, St. Louis, MO) to make solutions containing 1% w/v. These solutions were then mixed in a 2:2:1 ratio by volume, respectively, for immediate use.

2.4. In situ patterning of organoids

Organ-specific tissue constructs were biofabricated serially in individual predetermined chambers of the microfluidic device prior to sealing them. Either individual cells or spheroids were suspended within a 5 μL volume of the ECM-mimicking HA/gelatin-based hydrogel precursor, which was then introduced manually to the chamber and photocrosslinked by ultraviolet light exposure (BlueWave 200, Dymax, Torrington, CT) for 1 s with intensity of 1 W/cm^2 (Fig 1b). The vascular organoids in particular were exposed for only 0.25 s at the same intensity. The cell density or quantity of spheroids used to bioengineer the different tissue organoids was selected to coincide roughly with physiological *in vivo* tissue, with some variations incurred due to spheroid or cell availability. In the 3-organoid system, the first chamber contained 50 liver spheroids, the second chamber contained 10 cardiac spheroids, and the third chamber contained a lung organoid composed of A549 cells suspension at a density of 36 × 1010^6 cells/mL. In the 6-organoid system, the first two chambers again contained 50 liver spheroids and 10 cardiac spheroids, respectively. The third chamber contained 10 lung spheroids, followed by the fourth chamber which contained a vascular organoid composed of HUVECs in a suspension of 4 × 1010^6 cells/mL. The fifth chamber contained 10 brain spheroids, and finally the sixth chamber contained four testicular organoids. In all cases, organoids were photopatterned sequentially with only one construct exposed to UV at a time.

2.5. Experimental setup

Following organoid biofabrication, the device was immediately sealed with a prefabricated PMMA lid featuring fixed inlet and outlet ports fitted with PTFE tubing (Corning, Inc., Corning, NY). The inlet tubing of each device was connected to a media reservoir through a metal coupler (Instech, Plymouth, PA) and the outlet tubing was connected through a second coupler to 2-stop PVC 0.51 mm ID tubing (Cole-Parmer, Vernon Hills, IL). The loop was closed with a third coupler between the reservoir inlet and the free side of the PVC tubing. Media recirculation was achieved through mounting of the 2-stop braces through a micro-peristaltic pump (MP2 Precision, Elemental Scientific, Inc., Omaha, NE) operating at rate of 4 μL/min (Fig. 1c). The media reservoir was filled with 2 mL of common media formulation, which consisted of testis organoid media and EGM media (with supplements, but without FBS) mixed in a 1:1 ratio by volume. All devices were allowed to stabilize and prime the common media for at least two weeks to establish a baseline interaction between organs. For all systems, three conditions were investigated: Control: with liver, without drug; Condition 1: with liver, with drug; Condition 2: without liver, with drug. For the 6-organoid system, one chip was used as a Control and two more chips each for Conditions 1 & 2, respectively. After 14 days of incubation, the liver organoid chamber was removed from Condition 2 devices by connecting the media reservoir coupler directly to the cardiac inlet. Drug for both Condition 1 and 2 was introduced through media replenishment to the corresponding reservoirs. To ensure both high viability of the constructs and consistent drug concentration, the reservoirs were refreshed with clean common media (with or without drug) every two days. All the systems were sacrificed on day 21 and assessed for overall viability and targeted drug impact.

2.6. Preparation of drug stock solutions

Both capecitabine (a 5-fluorouracil prodrug) and ifosfamide (a nitrogen mustard containing chemotherapy prodrug) were obtained commercially (SML0653 and I4909, Sigma Aldrich). A 10 mM stock solution of capecitabine in DMSO which was then reconstituted in media to reach 20 μM concentration with 0.2% DMSO. A 1 mM stock solution of ifosfamide was prepared directly in media.

2.7. LIVE/DEAD cell viability

Cell viability was assessed by LIVE/DEAD (L/D) assay. Briefly, the stain solution was made by preparing 2 μM calcein-AM and 2 μM ethidium homodimer-1 (L/D Viability/Cytotoxicity Kit for mammalian cells, L3224, Thermo Fisher, Waltham, MA) in a 1:1 mixture of DMEM and PBS. Each multi-organoid system was flushed with clean PBS before introducing the L/D solution into the channels. The system reservoir of each chip was reconditioned with 500 μL of L/D solution and incubated for 1 hr under flow as above to maximize diffusion of the fluorescent dyes into the organoids. The channels were flushed again with PBS before *in situ* imaging with an Olympus FluoView™ FV1000 confocal microscope. 5 μm z-stacks of each organoid were obtained using 405 nm (green) and 559 nm (red) fluorescence filters. Images from these channels were then overlaid to produce a maximum projection image with calcein AM (green fluorescence) indicating live cells and ethidium homodimer (red fluorescence) indicating dead cells. Cell viability of individual spheroids or organoids were quantified using Imaris MeasurementPro software (Bitplane, Concord, MA) as described previously [16] by comparing the total number of cells in the green channel to the combined total number of cells in both the green and red channel.

2.8. Statistical analysis

Each experimental condition was investigated at least in duplicate except the 6-organoid control condition due to limited availability of cells. Viability was calculated as the mean ± the standard deviation between replicates. For hydrogel suspension organoids,

Please cite this article as: S.A.P. Rajan, J. Aleman and M. Wan et al., Probing prodrug metabolism and reciprocal toxicity with an integrated and humanized multi-tissue organ-on-a-chip platform, Acta Biomaterialia, https://doi.org/10.1016/j.actbio.2020.02.015

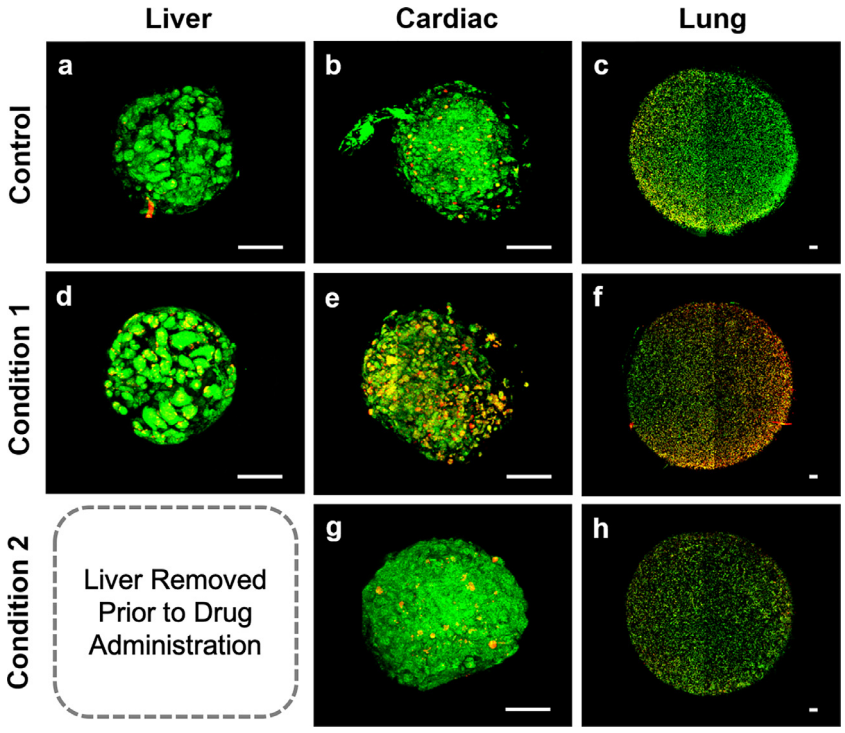

Fig. 2. Drug toxicity assessment of capecitabine in a 3-organoid system. L/D imaging of liver, cardiac, and lung organoids under Control (no drug, *a–c*), Condition 1 (with capecitabine and liver organoid, *d–f*), and Condition 2 (with capecitabine and without liver organoid, *g and h*). In Condition 1, the metabolized drug caused downstream toxicities in cardiac and lung organoids; in Condition 2, no significant toxicity occurred. Green stain: calcein AM-stained viable cells; Red stain: ethidium homodimer 1-stained dead cells. Scale bar represents 100 μM. (For interpretation of the references to colour in this figure legend, the reader is referred to the web version of this article.)

the whole construct was analyzed. For spheroid organoids, at least three co-incubated spheroids in each construct were analyzed collectively. The significant differences between the means were determined using Student's *t*-tests with confidence intervals of 95% or p-value <0.05.

3. Results and discussion

3.1. Implementation of a high viability 3-tissue platform with drug assessment

Our group has previously reported on a 3-tissue integrated model with liver, cardiac, and lung, in which each of these tissue models were extensively characterized [28]. This previous system consisted of three independent fluidic devices, each containing a single organoid or tissue construct. These organoids were produced with multiple biofabrication methods and were integrated by connecting the devices via PTFE tubing to establish a closed circulatory perfusion system. One particular drawback of this device architecture was its bulkiness, requiring large fluid and cell volumes that made it difficult to employ for high-throughput screening. It also featured non-physiological media-to-cell ratio (*i.e.* larger media volume compared to cell volume than the blood-to-tissue volume in humans), which may have pharmacological implications. Finally, the use of PDMS as a fabrication material creates potential obstacles in terms of adsorption of signaling molecules and even drugs.

One of the goals of the current study was to develop a low-cost microfluidic device that is both easy to fabricate and faithfully reproduces the complex interactions of drugs within the human body. As a first step, we fabricated the multi-organoid chip by rapid prototyping of adhesive films that were subsequently layered between glass and PMMA substrates to form an enclosed microfluidic device. In our system, we estimate that the surface area of each chamber is composed of ~42.5% PMMA, ~42.5% glass, and only ~15% adhesive film. This becomes advantageous for long-term experiments by reducing the effects of evaporation and non-specific adsorption through the surface of the device itself. Furthermore, the use of glass and PMMA thermoplastic provides high mechanical strength and optical transparency in the visible light range [39,40], allowing easy access to direct imaging of the organoids. Glass and PMMA are also less hydrophobic than typical materials like PDMS [41], and therefore reduce the adsorption of hydrophobic molecules to the interior channels, which can be a major drawback in PDMS-based devices. A current trend in organ-on-a-chip systems is transitioning towards other thermoplastics like cycloolefin (co)polymer (COC/COP) [13], polycarbonate [25], and polysulfone plastics [30,42] that are generally computer micromachined or commercially fabricated, thus requiring thermal or solvent-based bonding if not clamped using screws. The AFB device fabrication method allows the microfluidic devices to be produced rapidly, allowing device designs to be iterated quickly and optimized, and provides intrinsic bonding via the adhesive films.

The system was designed with simple fluid dynamics to achieve uniform velocity. In addition, the hydrogel matrix shielded fluid flow and reduced the fluid shear stress on the cells within the organoids. This mitigated any detrimental mechanical force effects while also increasing the time of exposure, interaction, and diffusion of the small volume of media to the organoids for maximum impact. Moreover, the AFB device accommodated a total fluid volume of less than 150 μL (~15 μL per individual chamber) to aid in conditioning the media during recirculation. Tissue volume was calculated to be approximately 17.3 μL, based on the average organoid size. From these values, we determined the tissue-to-liquid volume ratio on chip to be approximately 1:8.7, rivaling the lowest reported ratio used in any multi-organoid microphysiological system [43,44].

The individual chambers of the three-tissue chip contained ECM hydrogel matrices that encapsulated multiple tissue spheroids or

Please cite this article as: S.A.P. Rajan, J. Aleman and M. Wan et al., Probing prodrug metabolism and reciprocal toxicity with an integrated and humanized multi-tissue organ-on-a-chip platform, Acta Biomaterialia, https://doi.org/10.1016/j.actbio.2020.02.015

cells to emulate liver, heart, and lung tissues, respectively. We approached our 3D tissue modeling by implementing photopolymerization of the HA-based hydrogel precursor in the device (Fig. 1b) as it can be challenging to develop a spatially controlled 3D construct that is fabricated directly into a microfluidic system. We previously reported *in situ* biofabrication method of HA and gelatin hydrogels being photocrosslinked by PEGDA and a photoinitiator, yielding rapid gelation kinetics and improved spatial control over construct formation within the device [16,31,45,46]. Compared to traditionally used collagen, alginate, or Matrigel-based hydrogel scaffolds that rely on relatively slow or uncontrolled crosslinking kinetics, this photopolymerizing hydrogel allows both spheroids and cells to be encapsulated in the desired chambers nearly instantaneously through thiol-ene crosslinking. This method not only improved the efficiency in biofabricating tissue organoids, but also reproduced several aspects of native ECM and provided thoroughly tested hydrogel properties like cytocompatibility, elastic modulus, and porosity [18,31,47–49].

The 3-organoid systems were initially connected to reservoirs with 2000 µL of common organoid media recirculated in a closed loop and used to assess the long-term viability of the all cells. Each chamber was sequentially and externally interconnected via PTFE tubing to form an integrated system. The flow of the media into the device was initiated through the liver organoid chamber followed by the cardiac and lung tissue chambers. The ratios of functional liver and cardiac spheroids immobilized in each chamber were approximately 50 liver spheroids to approximately 10 cardiac spheroids, thus simulating the 5:1 ratio of liver to heart in terms of mass [50]. Both spheroid types have been validated thoroughly for organ-like functionality through a variety of immunological, metabolic, and drug response assays [28,47]. The third tissue type was the lung construct fabricated by photocrosslinking the hydrogel precursor with suspended A549 cells at a density to provide approximately the same cellular mass as the liver constructs, thereby simulating the nearly 1:1 ratio of liver to lung in terms of mass [51].

The platform was set under continuous perfusion of common organoid media that contained 1:1 ratio of serum-free endothelial cell media and testicular cell media that flowed through the chambers at 4 µL/min flow rate. Note that the media formulation of the common media (1:1 ratio of serum-free endothelial cell media and testicular cell media) was established based on ongoing parallel studies used to optimize cell culture media for augmented 6-tissue systems (described below). The viability of the organoids in the system was analyzed by L/D assay after 21 days. The maximum projection images acquired by confocal microscopy (Fig. 2a–c) demonstrated high viability of over 80% for all three organoid types (Fig. 3), showing that cell viability could be maintained in an integrated fashion in our system for extended periods.

Administration of targeted drug compounds can cause a given tissue or organ to secrete cytokines or produce metabolites that have downstream effects on other tissue types. In one of our previous studies, dependent and independent enzymatic-activation of 5-fluorouracil (5-FU) cardiotoxicity impact was reproduced, where damage to the cardiac organoid was observed exclusively in the presence of a healthy liver organoid [20]. Capecitabine is an oral prodrug that is converted into its active metabolite by a three-step process. The drug is metabolized into 5′-deoxy-S-fluorocytidine (5′-DFCR) by carboxylesterase and then to 5′-deoxy-S-fluorouridine (5′-DFUR) by cytidine deaminase. These two steps take place in the liver and the enzyme thymidine phosphorylase – which is found in higher levels in liver compared to other tissues – converts it into the active metabolite 5-FU [52,53], which is itself commonly used as a chemotherapeutic. Cardio toxicity has been reported in patients receiving 5-FU treatment, and during the course of such therapies, patients are recommended to monitor for cardiac abnormalities [54]. There have also been reported cases of pulmonary fibrosis developing during 5-FU therapy [55].

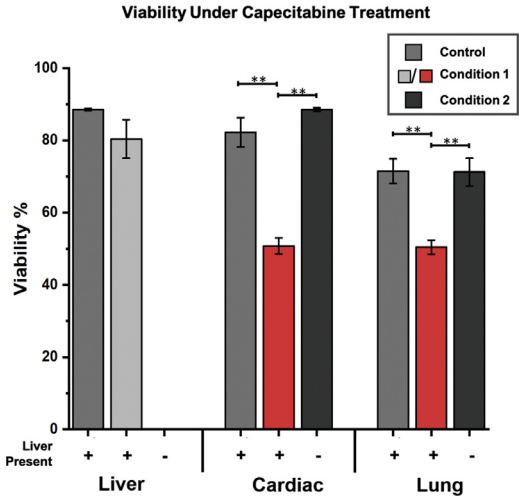

Fig. 3. Viability quantification under insult by capecitabine in a 3-organoid system. Quantification of live cell ratios (L/L + D) for liver, cardiac, and lung organoids under Control (no drug), Condition 1 (drug with liver organoid), and Condition 2 (drug without liver organoid). Reductions in viability are observed for both cardiac and lung organoids under Condition 1 (red). Statistical significance: ** $p < 0.05$. (For interpretation of the references to colour in this figure legend, the reader is referred to the web version of this article.)

To recapitulate this physiological process, we first allowed the 3-tissue system to be stabilized under the conditioned media for 14 days prior to adding 20 µM drug to the system. This allowed to stabilize the organoids and prime the common media to establish a baseline on all organoids systems. The 3-organoid system was then exposed to capecitabine by infusion into the common media. This concentration was chosen based on previous studies using 5-FU in the context of a different set of liver and tumor organoid models [56–59]. On day 7 after the prodrug was added (day 21 in total), the viability of the individual organoids was assessed by L/D staining and imaged by confocal microscopy. Following capecitabine exposure, we observed a qualitative reduction in cell viability in both the cardiac and the lung organoid (Fig. 2e-f). Indeed, L/D quantification revealed a 38.3% decrease in cardiac cell viability and a 37.1% decrease in lung cell viability compared to control conditions (Fig. 3). This cardiac and lung toxicity was consistent with the established capacetabine metabolism pathway [20,51], suggesting that the prodrug was converted into 5-FU by the liver organoid.

To validate that the effects were a result of these integrated tissue interactions, we repeated the experiment, but removed the liver organoid from circulation after the 14 days baseline period and before the capecitabine introduction. Without the liver, capecitabine should not be metabolized and converted to the active 5-FU compound, providing a negative control to the study. In this scenario, we hypothesized that there should not be downstream toxicity in the cardiac or lung organoids. We were able to confirm this prediction, finding no significant viability difference in the cardiac or lung organoids compared to control (Fig. 2g and h), in contrast to observations under the same prodrug conditions with the integrated liver organoid. These data corroborate that the prodrug capecitabine can be metabolized by a liver organoid into the 5-FU *in vitro*, as has been reported.

3.2. Implementation of a high viability 6-organoid platform with drug assessment

Following demonstration of 3-tissue organoid integration, the device was extended to incorporate additional tissue types in a

single platform to further enable testing of multi-tissue interactions following drug treatment. To this end, we sought next to integrates six different tissues, including liver, heart, lung, endothelium, brain, and testis. To further miniaturize and improve the media-to-cell ratio, all chambers were internally connected through narrow channels at equidistant positions, except for the liver chamber, which remained connected through external tubing to facilitate rerouting of media flow as in the 3-organoid system above. The revised pattern allowed us to decrease the working volume of media inside the chip itself significantly to less than 200 µL total; an increase of only 33% compared to the 3-organoid device despite doubling the number of organoid chambers. This ultimately improved the tissue-to-liquid volume ratio inside the chip to be 1:4.7. While still significantly different than the physiological 4:1 ratio of tissue:extracellular fluid found in humans [43], this is the most physiological ratio reported to date. This further concentrates the metabolites and cytokines released by each organoid and better conditions the environment, allowing for a more *in vivo*-like integrated system [25,50,60,61].

Like the 3-organoid device, this 6-organoid BOC system was entirely human-derived, incorporating human primary cells and iPS-derived cells. The first and second chamber contained liver and cardiac spheroids in the same ratio as above. Next, the lung module was represented by 8 −10 lung spheroids, followed by a vascular organoid assembled from HUVECs encapsulated in the HA hydrogel, then a brain organoid (10 brain spheroids), and finally a testis organoid (4 testis spheroids). The organoids are positioned in this order to emulate the *in vivo* blood flow to the organs [62–64]. Note that, like liver and heart above, the brain and testis spheroids have been characterized extensively with immunostaining and molecular assays to show physiological accuracy [36,37]. We note that while we accommodated a number of physiologically inspired features here (*e.g.* volume, organoid relative masses, etc.), one feature we did not include in the initial system was an accurate splitting of the fluid flow to different tissues that would parallel flow through the vasculature *in vivo*. This is a feature we continue to work towards. Additionally, while the fabrication and preparation of the devices used here for on-chip studies are relatively straightforward, we acknowledge that there are significant challenges in terms of infrastructure and planning to be able to incorporate a large number of cell- and tissue types in a single system. This level of complexity represents one limitation of our technology.

Once the 6-tissue system was assembled, the platform was maintained under continuous perfusion of common organoid media for 21 days before assessing for viability using L/D staining. The maximum projection images of stained organoids were acquired by confocal microscopy (Fig. 4a–f) and demonstrated >80% viability (Fig. 5). Though other multi-tissue platforms have established longer viability periods, those systems were largely 2D cell cultures or comprised only of cell lines in 3D [19,24,65]. Here, we have demonstrated viability of multiple human primary cells and iPS cell-based 3D organoids in a common media. We note that oxygen and nutrient levels were not measured to determine assess possible depletion. However, with viability levels above 80% for 3 weeks, we believe that these factors were not significant. ELISA and colorimetric tests conducted on the previous PDMS-based 3-organoid system probed biomarkers like IL-8 and IL-1β, and showed that these stress markers only spiked when the platform was subjected to chemical insult [28]. These data, combined with the 3- and 6-organoid systems described herein, suggest that the tissues condition the media through autocrine and paracrine signaling to generate a media that can support the bulk of the system in the same way that blood is capable of supporting the vastly integrated organ system that is the human body.

After establishing a stable baseline for 14 days under common media flow, we again introduced a drug compound: the prodrug ifosfamide, an alkylating antineoplastic agent [66]. Ifosfamide is a structural isomer of cyclophosphamide that has demonstrated efficacy in treating a wide range of tumors [67–69]. To be effective, the prodrug must be biotransformed to an active compound by cytochrome P-450 mixed-function oxidase enzymes that are primarily found in liver hepatocytes [51,70,71]. The ring hydroxylation of the drug eventually produces isophosphoramide mustard, which is the primary alkylating compound, along with the toxin acrolein. Hydroxylation also leads to increased alternative pathway metabolism that undergoes chloroethyl side chain oxidation resulting in the formation of alkylating metabolites such as chloracetaldehyde, which is known to further contribute to ifosfamide-induced neurotoxicity [66,72–74]. Indeed, lethal toxicity of ifosfamide toward 3D glial organoids has been reported in another microphysiological system [74].

To further validate our platform, we aimed to recapitulate this targeted toxicity *in vitro*. Following our 14-day incubation under common media, we introduced ifosfamide to systems either with (Condition 1) or without (Condition 2) the liver organoid in circulation. After 7 days of exposure to 1 mM ifosfamide [51,53,74], we analyzed the viability of the organoids using L/D assays as described above. From the maximum projection images, an apparent reduction in brain organoid viability was observed under Condition 1 (Fig. 4k) even while no such change was observed under Condition 2 (Fig. 4p). Consequently, ifosfamide exhibits significant neurotoxicity in the presence of liver organoids, implying hepatic P-450 metabolic activity and conversion of the drug into the neurotoxin chloracetaldehyde. To quantify cytoxicity, viability was determined from Z stacks of the L/D signals. Fig. 5 shows the viability of all organoids with or without ifosfamide and/or liver. Indeed, Condition 1 brain organoid viability (48.8%) is substantially less than that of the control system (72.4%) while the Condition 2 viability (72.9%) is not significantly different. No obvious differences were observed in any other organoids relative to their Controls.

Bioavailability of a drug determines the amount of circulating drug into the body that remains active for an established period of time. In this way, drug efficacy is directly related to bioavailability. Oral bioavailability of ifosfamide has been reported to be between 1.04 and 0.95 h for patients receiving 1 g/m^2 and 2 g/m^2 ifosfamide, respectively [76]. Portrayals of bioavailability on-chip have been attempted by dividing the mortality ratio of a control to the mortality ratio of a system with disrupted physiology in the presence of drug [51], similar to our no-liver condition. We note that more accurate empirical methods of evaluating bioavailability, including mass spectrometry, would increase the quantitative accuracy of our results. However, this approach would be challenging to incorporate with our system given the small fluid volumes used. The mortality ratio method described here, while more speculative in nature, allows an initial consideration of bioavailability in this system. The ratio of mortality in our control system (27.7%) divided by that found in Condition 1 (51.2%) yields an approximate ifosfamide bioavailability of 0.53. However, when the control is divided by the mortality ratio in Condition 2 (27.2%), giving 1.01 for the same time period. These results reinforce the idea that circulating ifosfamide in our system needs liver-associated metabolism to be neurologically toxic; while the Condition 2 systems had the drug in circulation, its efficacy was null as it required enzymatic activity to be damaging to the neural organoid. It should be noted that the cell-staining method using L/D is one of the most common methods for measuring cellular viability and death, but more precise methods for validation of this toxicity could be applied in the future, using assays to measure outcomes such as necrosis or apoptosis through immunostaining, ELISAs, RNA inhibition

Please cite this article as: S.A.P. Rajan, J. Aleman and M. Wan et al., Probing prodrug metabolism and reciprocal toxicity with an integrated and humanized multi-tissue organ-on-a-chip platform, Acta Biomaterialia, https://doi.org/10.1016/j.actbio.2020.02.015

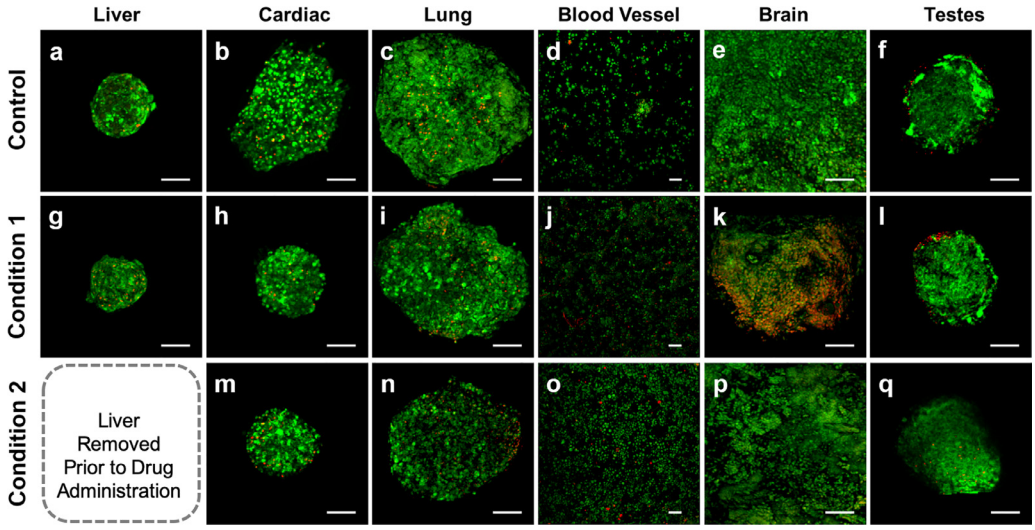

Fig. 4. Drug toxicity assessment of ifosfamide in a 6-organoid system. L/D imaging of liver, cardiac, lung, endothelial, brain, and testis organoids under Control (no drug, *a–c*), Condition 1 (with ifosfamide and liver organoid, *d–f*), and Condition 2 (with ifosfamide and without liver organoid, *g and h*). In Condition 1, the metabolized drug caused downstream toxicity in the brain organoid; in Condition 2, no significant toxicity occurred. Green stain: calcein AM-stained viable cells; Red stain: ethidium homodimer 1-stained dead cells. Scale bar represents 100 μM. (For interpretation of the references to colour in this figure legend, the reader is referred to the web version of this article.)

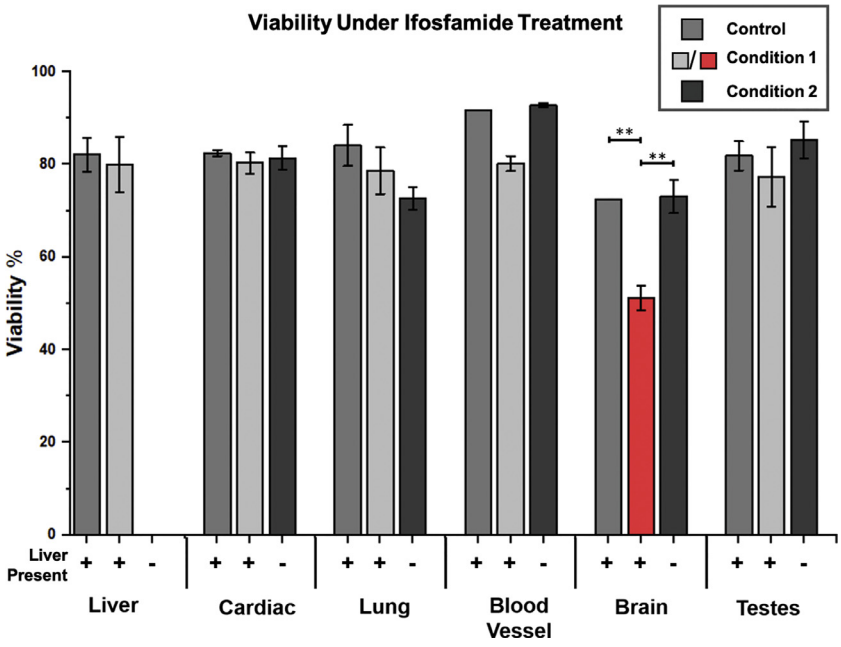

Fig. 5. Viability quantification under insult by ifosfamide in a 6-organoid system. Quantification of live cell ratios (L/L + D) for liver, cardiac, lung, endothelial, brain, and testis organoids under Control (no drug), Condition 1 (drug with liver organoid), and Condition 2 (drug without liver organoid). A significant reduction in viability is observed for the brain organoid under Condition 1 (red). Statistical significance: ** $p < 0.05$. (For interpretation of the references to colour in this figure legend, the reader is referred to the web version of this article.)

quantification, and dosage-dependent toxicity. In addition, investigations using metabolomics and proteomics to characterize total system function would be useful to gain a more comprehensive look at these systems, as would genomic assessments to determine whether cells in the system experience genetic drift or phenotypic changes *in vitro*. However, our approach provides an initial indication of the interactions that occur between organoids on chip. By replicating well-understood, metabolically-dependent, and targeted toxicity events in our 3- and 6-organoid systems, we have advanced towards a clinically relevant human system.

Lastly, one additional limitation of this platform is the representation of the vascular component. The platform described herein employed encapsulated endothelial cells, not a vascular network. It is possible that given time and additional signals such as growth factor loading, the cells might reorganize into a network, but in this scenario, this did not occur. We acknowledge that this is a limitation of our current system. We included endothelial cells as a representation of vascular biology rather than structure, but agree that it could be considered somewhat artificial. Our ultimate goal here was to show examples of integrated drug response where the presence or lack of drug metabolism influences other tissues when drugs are administered. We believe that the inclusion of endothelial cells even without the critical structures they form *in vivo* served this purpose. That being said, we aim to improve on the structure and function of the vascular component of the platform in ongoing studies.

Please cite this article as: S.A.P. Rajan, J. Aleman and M. Wan et al., Probing prodrug metabolism and reciprocal toxicity with an integrated and humanized multi-tissue organ-on-a-chip platform, Acta Biomaterialia, https://doi.org/10.1016/j.actbio.2020.02.015

4. Conclusion

The primary goal of this study was to develop a functional and physiologically-relevant multi-tissue organ-on-a-chip system with six integrated tissue types. To this end, we demonstrated the viability of both a 3- and a 6-organoid system, each operated in a common recirculating media for at least 21 days. Once these systems were established, functional drug responses were tested using capecitabine and ifosamide, respectively. As hypothesized, the integrated nature of the system was critical: when exposed to these drugs with the liver present, each was metabolized into a product with downstream toxicity in other organoids (cardiac, lung, or brain tissues, depending on the particular drug) while removal of the liver from the system resulted in no significant toxicity response in any tissue type. These results show how a single platform consisting of combinations of organoids can create a more complex and integrated response where the functionality of one organoid influences the response of others.

In addition, we demonstrate the utility of *in situ* photopatterning 3D tissue constructs inside closed microfluidic devices using a photosensitive ECM-derived hydrogel matrix with a versatility that can be expanded to a variety of applications. For example, the photopatterning technique can be expanded to multi-step spatial patterning of selective zones of particular cells or ECM compositions, creating more complex constructs, an approach we are using in other ongoing research. Furthermore, the chemistry behind the hydrogel components supports addition of other ECM factors that can deliver a more faithful mimic of native tissue ECM. Along with HA, gelatin, and heparin that are already present, additional ECM components like chemically modified laminin and fibronectin, growth factors, and other cytokines can be included via direct covalent bonding or heparin-modulated binding. The versatility of this biofabrication method is currently being utilized to model healthy and diseased tissues with multi-domain structures thus emulating essential *in vivo* structural and physiological components.

A typical concern with 3D systems in general is whether they perform significantly better than 2D systems. While 2D cell cultures have yielded invaluable data and discoveries, there is a growing body of work demonstrating that in many cases 3D organoids and other models of increased complexity may be a superior technology overall. For example, we have previously reported significant differences in critical aspects like liver functionality [18], accuracy of phenotypes in cancer cell models [59,75], and drug screening differences [58]. These results are part of a growing body of work demonstrating the advantages of 3D culture compared to 2D.

With multi-organoid integration, our system exemplifies an important capability *in vitro* drug and toxicology screening and disease modeling. We anticipate that future iterations of this platform and others like it will be important drivers of drug development efforts, allowing for more accurate, human-based drug response data to be collected and ultimately reducing costs and improving the chances of success for novel drug compounds.

Declaration of Competing Interest

The authors have no conflicts of interest to disclose.

Acknowledgements

The authors gratefully acknowledge funding by the Defense Threat Reduction Agency (DTRA) under Space and Naval Warfare Systems Center Pacific (SSC PACIFIC) Contract No. N6601-13-C-2027. The publication of this material does not constitute approval by the government of the findings or conclusions herein.

References

[1] J. Arrowsmith, Trial watch: phase III and submission failures: 2007-2010, Nat. Rev. Drug. Discov. 10 (2) (2011) 87.
[2] M. Allison, Clinical setbacks reduce IGF-1 inhibitors to cocktail mixers, Nat. Biotechnol. 30 (10) (2012) 906–907.
[3] G. Pretorius, Phase III trial failures: costly, but preventable, Appl. Clin. Trials. 25 (8) (2016).
[4] H.R. Ferdowsian, N. Beck, Ethical and scientific considerations regarding animal testing and research, PLoS ONE 6 (9) (2011) e24059.
[5] K. Duval, H. Grover, L.H. Han, Y. Mou, A.F. Pegoraro, J. Fredberg, Z. Chen, Modeling physiological events in 2D *vs.* 3D cell culture, Physiology (Bethesda) 32 (4) (2017) 266–277.
[6] D. Huh, G.A. Hamilton, D.E. Ingber, From 3D cell culture to organs-on-chips, Trends Cell Biol 21 (12) (2011) 745–754.
[7] M. Devarasetty, A.R. Mazzocchi, A. Skardal, Applications of bioengineered 3D tissue and tumor organoids in drug development and precision medicine: current and future, BioDrugs 32 (1) (2018) 53–68.
[8] A. Skardal, T. Shupe, A. Atala, Organoid-on-a-chip and body-on-a-chip systems for drug screening and disease modeling, Drug Discov. Today 21 (9) (2016) 1399–1411.
[9] K.H. Benam, S. Dauth, B. Hassell, A. Herland, A. Jain, K.J. Jang, K. Karalis, H.J. Kim, L. MacQueen, R. Mahmoodian, S. Musah, Y.S. Torisawa, A.D. van der Meer, R. Villenave, M. Yadid, K.K. Parker, D.E. Ingber, Engineered *in vitro* disease models, Annu. Rev. Pathol. 10 (2015) 195–262.
[10] D. Huh, B.D. Matthews, A. Mammoto, M. Montoya-Zavala, H.Y. Hsin, D.E. Ingber, Reconstituting organ-level lung functions on a chip, Science 328 (5986) (2010) 1662–1668.
[11] A. Polini, L. Prodanov, N.S. Bhise, V. Manoharan, M.R. Dokmeci, A. Khademhosseini, Organs-on-a-chip: a new tool for drug discovery, Expert Opin. Drug Discov. 9 (4) (2014) 335–352.
[12] N.S. Bhise, J. Ribas, V. Manoharan, Y.S. Zhang, A. Polini, S. Massa, M.R. Dokmeci, A. Khademhosseini, Organ-on-a-chip platforms for studying drug delivery systems, J. Control Release 190 (2014) 82–93.
[13] J. Theobald, A. Ghanem, P. Wallisch, A.A. Banaeiyan, M.A. Andrade-Navarro, K. Taškova, M. Haltmeier, A. Kurtz, H. Becker, S. Reuter, R. Mrowka, X. Cheng, S. Wölfl, Liver-Kidney-on-Chip to study toxicity of drug metabolites, ACS Biomater. Sci. Eng. 4 (1) (2018) 78–89.
[14] Y.S. Zhang, A. Arneri, S. Bersini, S.R. Shin, K. Zhu, Z. Goli-Malekabadi, J. Aleman, C. Colosi, F. Busignani, V. Dell'Erba, C. Bishop, T. Shupe, D. Demarchi, M. Moretti, M. Rasponi, M.R. Dokmeci, A. Atala, A. Khademhosseini, Bioprinting 3D microfibrous scaffolds for engineering endothelialized myocardium and heart-on-a-chip, Biomaterials 110 (2016) 45–59.
[15] A. Agarwal, J.A. Goss, A. Cho, M.L. McCain, K.K. Parker, Microfluidic heart on a chip for higher throughput pharmacological studies, Lab. Chip 13 (18) (2013) 3599–3608.
[16] A.R. Mazzocchi, S.A.P. Rajan, K.I. Votanopoulos, A.R. Hall, A. Skardal, *In vitro* patient-derived 3D mesothelioma tumor organoids facilitate patient-centric therapeutic screening, Sci. Rep. 8 (1) (2018) 2886.
[17] P. Loskill, S.G. Marcus, A. Mathur, W.M. Reese, K.E. Healy, muOrgano: a Lego(R)-like plug & play system for modular multi-organ-chips, PLoS ONE 10 (10) (2015) e0139587.
[18] A. Skardal, S.V. Murphy, M. Devarasetty, I. Mead, H.W. Kang, Y.J. Seol, Z.Y. S., S.R. Shin, L. Zhao, J. Aleman, A.R. Hall, T. Hartung, A. Khademhosseini, S. Soker, C.E. Bishop, A. Atala, Multi-tissue interactions in an integrated three-tissue organ-on-a-chip platform, Sci. Rep. 7 (2017) 8837.
[19] C.D. Edington, W.L.K. Chen, E. Geishecker, T. Kassis, L.R. Soenksen, B.M. Bhushan, D. Freake, J. Kirschner, C. Maass, N. Tsamandouras, J. Valdez, C.D. Cook, T. Parent, S. Snyder, J. Yu, E. Suter, M. Shockley, J. Velazquez, J.J. Velazquez, L. Stockdale, J.P. Papps, I. Lee, N. Vann, M. Gamboa, M.E. LaBarge, Z. Zhong, X. Wang, L.A. Boyer, D.A. Lauffenburger, R.L. Carrier, C. Communal, S.R. Tannenbaum, C.L. Stokes, D.J. Hughes, G. Rohatgi, D.L. Trumper, M. Cirit, L.G. Griffith, Interconnected microphysiological systems for quantitative biology and pharmacology studies, Sci. Rep. 8 (1) (2018) 4530.
[20] Y.S. Zhang, J. Aleman, S.R. Shin, T. Kilic, D. Kim, S.A. Mousavi Shaegh, S. Massa, R. Riahi, S. Chae, N. Hu, H. Avci, W. Zhang, A. Silvestri, A. Sanati Nezhad, A. Manbohi, F. De Ferrari, A. Polini, G. Calzone, N. Shaikh, P. Alerasool, E. Budina, J. Kang, N. Bhise, J. Ribas, A. Pourmand, A. Skardal, T. Shupe, C.E. Bishop, M.R. Dokmeci, A. Atala, A. Khademhosseini, Multisensor-integrated organs-on-chips platform for automated and continual *in situ* monitoring of organoid behaviors, Proc. Natl. Acad. Sci. U S A 114 (12) (2017) E2293–E2302.
[21] M.L. Shuler, Organ-, body- and disease-on-a-chip systems, Lab Chip 17 (14) (2017) 2345–2346.
[22] J.P. Wikswo, E.L. Curtis, Z.E. Eagleton, B.C. Evans, A. Kole, L.H. Hofmeister, W.J. Matloff, Scaling and systems biology for integrating multiple organs-on-a-chip, Lab. Chip. 13 (18) (2013) 3496–3511.
[23] M.B.E. Michael, L. Shuler, Body-on-a chip: using microfluidic systems to predict human responses to drugs, Pure and Appl. Chem. 82 (8) (2010) 1635–1645.
[24] C. Oleaga, A. Riu, S. Rothemund, A. Lavado, C.W. McAleer, C.J. Long, K. Persaud, N.S. Narasimhan, M. Tran, J. Roles, C.A. Carmona-Moran, T. Sasserath, D.H. Elbrecht, L. Kumanchik, L.R. Bridges, C. Martin, M.T. Schnepper, G. Ekman, M. Jackson, Y.I. Wang, R. Note, J. Langer, S. Teissier, J.J. Hickman, Investigation of the effect of hepatic metabolism on off-target cardiotoxicity in a multi-organ human-on-a-chip system, Biomaterials 182 (2018) 176–190.

Please cite this article as: S.A.P. Rajan, J. Aleman and M. Wan et al., Probing prodrug metabolism and reciprocal toxicity with an integrated and humanized multi-tissue organ-on-a-chip platform, Acta Biomaterialia, https://doi.org/10.1016/j.actbio.2020.02.015

[25] P.G. Miller, M.L. Shuler, Design and demonstration of a pumpless 14 compartment microphysiological system, Biotechnol. Bioeng. 113 (10) (2016) 2213–2227.
[26] A.G. Jannick Theobald, P. Wallisch, A.A. Banaeiyan, M.A. Andrade-Navarro, K. Taškova, M. Haltmeier, A. Kurtz, H. Becker, S. Reuter, R. Mrowka, X. Cheng, S. Wölfl, Liver-Kidney-on-Chip to study toxicity of drug metabolites, ACS Biomater. Sci. Eng. 4 (1) (2018) 78–89.
[27] O. Frey, P.M. Misun, D.A. Fluri, J.G. Hengstler, A. Hierlemann, Reconfigurable microfluidic hanging drop network for multi-tissue interaction and analysis, Nat. Commun. 5 (2014) 4250.
[28] A. Skardal, S.V. Murphy, M. Devarasetty, I. Mead, H.W. Kang, Y.J. Seol, Y. Shrike Zhang, S.R. Shin, L. Zhao, J. Aleman, A.R. Hall, T.D. Shupe, A. Kleensang, M.R. Dokmeci, S. Jin Lee, J.D. Jackson, J.J. Yoo, T. Hartung, A. Khademhosseini, S. Soker, C.E. Bishop, A. Atala, Multi-tissue interactions in an integrated three--tissue organ-on-a-chip platform, Sci. Rep. 7 (1) (2017) 8837.
[29] J.H. Sung, Y.I. Wang, N. Narasimhan Sriram, M. Jackson, C. Long, J.J. Hickman, M.L. Shuler, Recent advances in body-on-a-chip systems, Anal. Chem. 91 (1) (2019) 330–351.
[30] W.L.K. Chen, C. Edington, E. Suter, J. Yu, J.J. Velazquez, J.G. Velazquez, M. Shockley, E.M. Large, R. Venkataramanan, D.J. Hughes, C.L. Stokes, D.L. Trumper, R.L. Carrier, M. Cirit, L.G. Griffith, D.A. Lauffenburger, Integrated gut/liver microphysiological systems elucidates inflammatory inter-tissue crosstalk, Biotechnol. Bioeng. 114 (11) (2017) 2648–2659.
[31] J. Aleman, A. Skardal, A multi-site metastasis-on-a-chip microphysiological system for assessing metastatic preference of cancer cells, Biotechnol. Bioeng. (2018).
[32] P.M. van Midwoud, A. Janse, M.T. Merema, G.M. Groothuis, E. Verpoorte, Comparison of biocompatibility and adsorption properties of different plastics for advanced microfluidic cell and tissue culture models, Anal. Chem. 84 (9) (2012) 3938–3944.
[33] N.P. Zarandi, G. Galdon, S. Kogan, A. Atala, H. Sadri-Ardekani, Cryostorage of immature and mature human testis tissue to preserve spermatogonial stem cells (SSCs): a systematic review of current experiences toward clinical applications, Stem Cells Cloning 11 (2018) 23–38.
[34] H. Sadri-Ardekani, M.A. Akhondi, F. van der Veen, S. Repping, A.M. van Pelt, *In vitro* propagation of human prepubertal spermatogonial stem cells, JAMA 305 (23) (2011) 2416–2418.
[35] H. Sadri-Ardekani, S.C. Mizrak, S.K. van Daalen, C.M. Korver, H.L. Roepers-Gajadien, M. Koruji, S. Hovingh, T.M. de Reijke, J.J. de la Rosette, F. van der Veen, D.G. de Rooij, S. Repping, A.M. van Pelt, Propagation of human spermatogonial stem cells *in vitro*, JAMA 302 (19) (2009) 2127–2134.
[36] S.S. Pendergraft, H. Sadri-Ardekani, A. Atala, C.E. Bishop, Three-dimensional testicular organoid: a novel tool for the study of human spermatogenesis and gonadotoxicity *in vitro*, Biol. Reprod. 96 (3) (2017) 720–732.
[37] G. Nzou, R.T. Wicks, E.E. Wicks, S.A. Seale, C.H. Sane, A. Chen, S.V. Murphy, J.D. Jackson, A.J. Atala, Human cortex spheroid with a functional blood brain barrier for high-throughput neurotoxicity screening and disease modeling, Sci. Rep. 8 (1) (2018) 7413.
[38] A. Skardal, L. Smith, S. Bharadwaj, A. Atala, S. Soker, Y. Zhang, Tissue specific synthetic ECM hydrogels for 3-D *in vitro* maintenance of hepatocyte function, Biomaterials 33 (18) (2012) 4565–4575.
[39] H. Becker, U. Heim, Hot embossing as a method for the fabrication of polymer high aspect ratio structures, Sens. Acta 83 (1) (2000) 130–135.
[40] C.-.W. Tsao, D.L.J.M. DeVoe, Nanofluidics, bonding of thermoplastic polymer microfluidics, 6(1) (2009) 1–16.
[41] K.S. Yun, E. Yoon, Fabrication of complex multilevel microchannels in PDMS by using three-dimensional photoresist masters, Lab. Chip. 8 (2) (2008) 245–250.
[42] N. Tsamandouras, W.L.K. Chen, C.D. Edington, C.L. Stokes, L.G. Griffith, M. Cirit, Integrated gut and liver microphysiological systems for quantitative in vitro pharmacokinetic studies, AAPS J. 19 (5) (2017) 1499–1512.
[43] E.M. Materne, I. Maschmeyer, A.K. Lorenz, R. Horland, K.M. Schimek, M. Busek, F. Sonntag, R. Lauster, U. Marx, The multi-organ chip–a microfluidic platform for long-term multi-tissue coculture, J. Vis. Exp. (98) (2015) e52526.
[44] E.M. Materne, A.G. Tonevitsky, U. Marx, Chip-based liver equivalents for toxicity testing–organotypicalness *versus* cost-efficient high throughput, Lab. Chip. 13 (18) (2013) 3481–3495.
[45] A. Skardal, M. Devarasetty, S. Soker, A.R. Hall, In situ patterned micro 3D liver constructs for parallel toxicology testing in a fluidic device, Biofabrication 7 (3) (2015) 031001.
[46] J. Aleman, S.K. George, S. Herberg, M. Devarasetty, C.D. Porada, A. Skardal, G. Almeida-Porada, Deconstructed microfluidic bone marrow on-a-chip to study normal and malignant hemopoietic cell-niche interactions, Small 15 (43) (2019) e1902971.
[47] S.D. Forsythe, M. Devarasetty, T.D. Shupe, C.E. Bishop, A. Atala, S. Soker, A. Skardal, Environmental toxin screening using human-derived 3D bioengineered liver and cardiac organoids, Frontiers in Public Health (2018) In press.
[48] A. Skardal, S.V. Murphy, K. Crowell, D. Mack, A. Atala, S. Soker, A tunable hydrogel system for long-term release of cell-secreted cytokines and bioprinted *in situ* wound cell delivery, J. Biomed. Mater. Res. B Appl. Biomater. (2016).
[49] A. Skardal, J. Zhang, G.D. Prestwich, Bioprinting vessel-like constructs using hyaluronan hydrogels crosslinked with tetrahedral polyethylene glycol tetracrylates, Biomaterials 31 (24) (2010) 6173–6181.
[50] T. Takebe, B. Zhang, M. Radisic, Synergistic engineering: organoids meet organs-on-a-chip, Cell Stem Cell 21 (3) (2017) 297–300.
[51] H. Kimura, T. Ikeda, H. Nakayama, Y. Sakai, T. Fujii, An on-chip small intestine-liver model for pharmacokinetic studies, J. Lab. Autom. 20 (3) (2015) 265–273.
[52] C.M. Walko, C. Lindley, Capecitabine: a review, Clin. Ther. 27 (1) (2005) 23–44.
[53] C.G. Yang, Y.F. Wu, Z.R. Xu, J.H. Wang, A radial microfluidic concentration gradient generator with high-density channels for cell apoptosis assay, Lab. Chip. 11 (19) (2011) 3305–3312.
[54] J.D. Sara, J. Kaur, R. Khodadadi, M. Rehman, R. Lobo, S. Chakrabarti, J. Herrmann, A. Lerman, A. Grothey, 5-fluorouracil and cardiotoxicity: a review, Ther. Adv. Med. Oncol. 10 (2018) 1758835918780140.
[55] A.K. Chan, B.A. Choo, J. Glaholm, Pulmonary toxicity with oxaliplatin and capecitabine/5-Fluorouracil chemotherapy: a case report and review of the literature, Onkologie 34 (8–9) (2011) 443–446.
[56] M. Devarasetty, A. Skardal, K. Cowdrick, F. Marini, S. Soker, Bioengineered submucosal organoids for in vitro modeling of colorectal cancer, Tissue Eng Part A 23 (19–20) (2017) 1026–1041.
[57] M. Devarasetty, E. Wang, S. Soker, A. Skardal, Mesenchymal stem cells support growth and organization of host-liver colorectal-tumor organoids and possibly resistance to chemotherapy, Biofabrication 9 (2) (2017) 021002.
[58] S. Forsythe, N. Mehta, M. Devarasetty, H. Sivakumar, W. Gmeiner, S. Soker, K. Votanopoulos, A. Skardal, Development of a colorectal cancer 3D micro–tumor construct platform from cell lines and patient tumor biospecimens for standard-of-care and experimental drug screening, Ann Biomed Eng (2019).
[59] A. Skardal, M. Devarasetty, C. Rodman, A. Atala, S. Soker, Liver-Tumor hybrid organoids for modeling tumor growth and drug response in vitro, Ann. Biomed. Eng. 43 (10) (2015) 2361–2373.
[60] J.H. Sung, M.B. Esch, J.M. Prot, C.J. Long, A. Smith, J.J. Hickman, M.L. Shuler, Microfabricated mammalian organ systems and their integration into models of whole animals and humans, Lab. Chip. 13 (7) (2013) 1201–1212.
[61] I. Wagner, E.M. Materne, S. Brincker, U. Sussbier, C. Fradrich, M. Busek, F. Sonntag, D.A. Sakharov, E.V. Trushkin, A.G. Tonevitsky, R. Lauster, U. Marx, A dynamic multi-organ-chip for long-term cultivation and substance testing proven by 3D human liver and skin tissue co-culture, Lab. Chip. 13 (18) (2013) 3538–3547.
[62] S.N. Bhatia, D.E. Ingber, Microfluidic organs-on-chips, Nat. Biotechnol. 32 (8) (2014) 760–772.
[63] J.H. Sung, B. Srinivasan, M.B. Esch, W.T. McLamb, C. Bernabini, M.L. Shuler, J.J. Hickman, Using physiologically-based pharmacokinetic-guided "body-on-a-chip" systems to predict mammalian response to drug and chemical exposure, Exp. Biol. Med. 239 (9) (2014) 1225–1239.
[64] S.H. Lee, J.H. Sung, Microtechnology-Based multi-organ models, Bioengineering 4 (2) (2017).
[65] C. Oleaga, C. Bernabini, A.S. Smith, B. Srinivasan, M. Jackson, W. McLamb, V. Platt, R. Bridges, Y. Cai, N. Santhanam, B. Berry, S. Najjar, N. Akanda, X. Guo, C. Martin, G. Ekman, M.B. Esch, J. Langer, G. Ouedraogo, J. Cotovio, L. Breton, M.L. Shuler, J.J. Hickman, Multi-Organ toxicity demonstration in a functional human *in vitro* system composed of four organs, Sci. Rep. 6 (2016) 20030.
[66] K.L. Dechant, R.N. Brogden, T. Pilkington, D. Faulds, Ifosfamide/mesna. A review of its antineoplastic activity, pharmacokinetic properties and therapeutic efficacy in cancer, Drugs 42 (3) (1991) 428–467.
[67] M. Zalupski, L.H. Baker, Ifosfamide, J. Natl. Cancer Inst. 80 (8) (1988) 556–566.
[68] M. Furlanut, L. Franceschi, Pharmacology of ifosfamide, Oncology 65 (Suppl 2) (2003) 2–6.
[69] R.B. Weiss, Ifosfamide *vs* cyclophosphamide in cancer therapy, Oncology (Williston Park) 5 (5) (1991) 67–76 discussion 76-82, 84-6.
[70] L. Choucha-Snouber, C. Aninat, L. Grsicom, G. Madalinski, C. Brochot, P.E. Poleni, F. Razan, C.G. Guillouzo, C. Legallais, A. Corlu, E. Leclerc, Investigation of ifosfamide nephrotoxicity induced in a liver-kidney co-culture biochip, Biotechnol Bioeng 110 (2) (2013) 597–608.
[71] R. Polimanti, S. Piacentini, D. Manfellotto, M. Fuciarelli, Human genetic variation of CYP450 superfamily: analysis of functional diversity in worldwide populations, Pharmacogenomics 13 (16) (2012) 1951–1960.
[72] P. Nicolao, B. Giometto, Neurological toxicity of ifosfamide, Oncology 65 (Suppl 2) (2003) 11–16.
[73] M.H. Cohen, P.J. Creaven, F. Tejada, H.H. Hansen, F. Muggia, A. Mittelman, O.S. Selawry, Phase I clinical trial of isophosphamide (NSC-109724), Cancer Chemother. Rep. 59 (4) (1975) 751–755.
[74] L. Ma, J. Barker, C. Zhou, W. Li, J. Zhang, B. Lin, G. Foltz, J. Kublbeck, P. Honkakoski, Towards personalized medicine with a three-dimensional micro-scale perfusion-based two-chamber tissue model system, Biomaterials 33 (17) (2012) 4353–4361.
[75] A. Skardal, M. Devarasetty, S. Forsythe, A. Atala, S. Soker, A reductionist metastasis-on-a-chip platform for *in vitro* tumor progression modeling and drug screening, Biotechnol. Bioeng. 113 (9) (2016) 2020–2032.
[76] T. Wagner, P. Drings, Pharmacokinetics and bioavailability of oral ifosfamide, Arzneimittelforschung 36 (5) (1986) 878–880.

Please cite this article as: S.A.P. Rajan, J. Aleman and M. Wan et al., Probing prodrug metabolism and reciprocal toxicity with an integrated and humanized multi-tissue organ-on-a-chip platform, Acta Biomaterialia, https://doi.org/10.1016/j.actbio.2020.02.015